ONSET, GROWTH, PROGRESSION AND UNIFORMITY OF SHEAR BANDS IN DILATIVE SANDS

Amy L. Rechenmacher
Department of Civil Engineering, Johns Hopkins University, USA

ABSTRACT

A non-destructive imaging-based displacement measurement technique, Digital Image Correlation (DIC), was used to evaluate local displacements on surfaces of sand specimens throughout biaxial and triaxial tests. The DIC method yielded thousands of displacement data points across an imaged surface of a specimen, providing the opportunity for analysis of local, micro-level displacement mechanisms that trigger the onset of persistent shear bands. The displacement patterns evidenced both in biaxial and triaxial tests suggested clearly that shear banding naturally initiates along conjugate planes. However, when test boundary conditions did not constrain shear band growth, the formation of a single, persistent shear band was favored; otherwise, conjugate shear was sustained. Shear band formation commenced just before peak stress, near the edges of the specimen, where shear deformation was least constrained. Shear band formation was not instantaneous, but required a finite amount of shear translation to fully initiate. Displacement gradients across shear bands were decidedly parabolic, and displacement fields along the length of a shear band exhibited a notable, non-rotational periodicity, perhaps associated with "force chain" buildup and collapse.

1 INTRODUCTION

Shear bands are a ubiquitous feature associated with post-peak response in dilative sands. Much experimental research on shear bands has been aimed at understanding patterns of shear banding within laboratory soil specimens (e.g. Harris et al [1]; Finno et al [2]; Desrues et al. [3]); volume change and geometric characteristics of persistent shear bands (e.g. Liang et al. [4]; Mooney et al. [5]; Finno and Rechenmacher [6]); and the overall effect of shear bands on constitutive response (e.g. Han and Drescher [7]; Alshibli et al. [8]). In contrast, experimental difficulties in capturing grain-scale deformations have limited study of displacement mechanisms that trigger the onset of localization and the character of displacement fields within persistent shear bands.

This paper describes results of experimental research utilizing Digital Image Correlation (DIC) to evaluate local displacements in dilative sands during biaxial and triaxial testing. The DIC method operates by matching pixel gray level values between digital images. By analyzing digital images acquired throughout testing, detailed, local specimen displacement information was obtained through the course of shear band onset, growth, and evolution. The nature and uniformity of displacements within shear bands also was investigated. Comparison of behavior between biaxial and triaxial specimens provided insight regarding the effects of loading mode as well as boundary conditions on shear banding in laboratory specimens.

2 EXPERIMENTAL METHODS

2.1 Laboratory Testing

Tests on axisymmetric specimens were conducted in a conventional triaxial compression apparatus using nonlubricated ends. Tests were performed under vacuum confinement, without use of the conventional Plexiglas confining cell, so as to avoid any potential distortion during digital imaging. The plane strain testing apparatus (Rechenmacher and Finno [9]) was designed to promote unconstrained shear band formation and growth (Drescher et al. [10]): the bottom of the

specimen rests within a one-way, low-friction, ball-bearing "sled", creating a lack of constraint such that shear band growth and propagation is uninhibited by boundary conditions. One of the plane strain wall is constructed of clear Plexiglas, providing a window for imaging in plane deformations.

Consolidated-drained compression tests were conducted on medium-dense and dense specimens of several different sands (Table 1). Specimens were prepared either using dry pluviation or vibratory densification in layers. Throughout the tests, high resolution (1 to 4 Megapixels) digital images were captured with low defect CCD cameras (e.g. Rechenmacher and Finno [9]). In the triaxial tests, images from two obliquely oriented cameras were taken simultaneously, to provide the stereo perspective required for 3D-DIC method (described below).

Table 1. Properties of Sands Tested in Biaxial or Triaxial Experiments

Sand Type	D_{50} (mm)	C_u	C_c	D_r (%)	p_c' (kPa)
Mason	0.32	1.3	1.02	78	350
Levering	0.49	1.47	1.14	92	40
Delaware Beach	0.40	1.26	1.00	76	150
Concrete	0.62	3.8	0.67	52	222

2.2 Digital Image Correlation (DIC)

The basis of DIC is the tracking of unique pixel gray-value patterns within small neighborhoods, or subsets, of a digital image: given an initially square subset of pixels, and a search is performed in a subsequent image to find the most optimal match (e.g. Sutton et al. [11]). Full-field displacement information is obtained by overlapping the pixel subsets. The DIC-based programs VIC-2D and VIC-3D, by Correlated Solutions, Inc., were used in the current research. The DIC algorithms utilize cubic-order and higher sub-pixel interpolation schemes, such that continuous intensity distributions are matched, and also accommodate the possibility of affine subset deformation. Collectively, these features enable displacement measurement to sub-pixel accuracy.

3D-DIC is based on principles similar to human depth perception: by viewing the same object from two different viewpoints, the precise three-dimensional shape of the object can be resolved (Helm et al. [12]). A calibration process is conducted prior to the start of each test, in which a dot-target is placed in the field of view, and a sequence of images is acquired for different orientations of the target. From these images, calibration parameters, including camera-based parameters such as focal length, image center and lens distortion, as well as the relative orientation of the two cameras in space, are computed. Once an object's shape is discerned, displacements between consecutive sets of images are computed using the DIC concepts described above.

The accuracy of DIC displacement measurement for sands tested within the biaxial apparatus was investigated by Rechenmacher and Finno [9]. Results indicated that displacements could be discerned to an accuracy of 0.08 pixels, or about +/- 0.01 mm for typical image scales.

3 EXPERIMENTAL RESULTS AND DISCUSSION

3.1 Onset of Persistent Localization in Dilative Sands

Figure 1 shows contours and vectors of incremental DIC displacements during a biaxial compression test on dense masonry sand. Image locations are indicated in the stress-strain curve. DIC analyses for this test produced over 10,000 displacement data points across the analysis area, which extended over about 80% of the specimen height and width (membrane discoloration and shadowing prevented analysis of the entire specimen face). About 3% of the subset displacement

vectors are shown for clarity. The scale bar and tick marks along the axes indicate 20-mm distances horizontally and vertically across the specimen face.

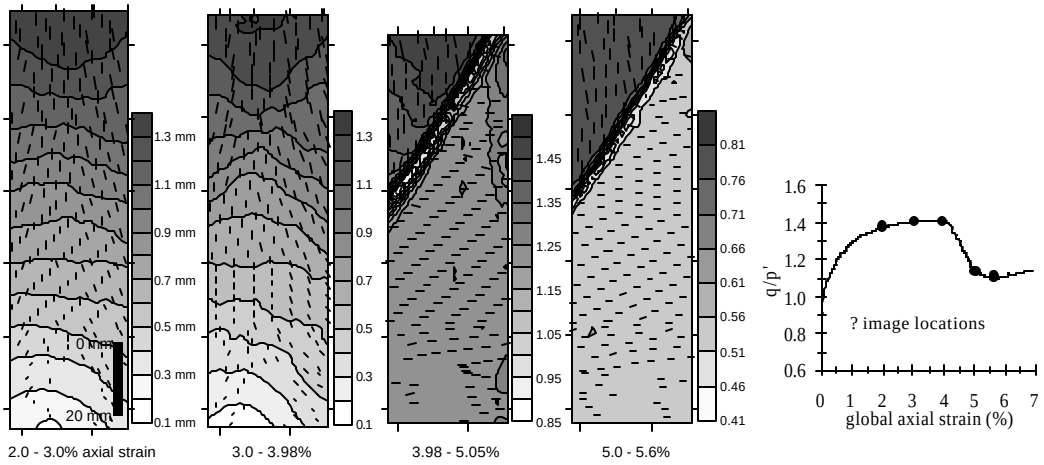

Figure 1. Local DIC-Derived Displacements During Biaxial Compression Test on Mason Sand.

The first analysis increment preceded the achievement of peak stress. Specimen strains were largely compressive and uniform across the specimen height (note that in spite of the use of platen lubrication, a slight amount of frictional resistance occurred). The next increment, 3.0 to 3.98% axial strain, just encompassed peak stress (3.92% axial strain). The back-to-back "V" zones of slightly more concentrated deformation at the upper third-point of the specimen suggests that localization is initializing along conjugate planes. By the 3.98 to 5.0% strain increment, the downward left of the two conjugate directions had evolved to a focused, linear zone of intense shear deformation, while a small amount of diffuse shear deformation remained in the conjugate direction. By 5.0% axial strain, the shear band is completely formed.

Figure 2 shows local displacements that occurred during a triaxial test on dense Levering sand. For clarity, only resolved x- and y-direction (horizontal and vertical) displacements are shown imposed over an x-y projection of the correlated portion of the specimen face (displacement measurements were obtained over about 90-degrees of the specimen circumference). Image locations are indicated on the stress-strain curve. The tendency toward conjugate localization is again seen. While one persistent shear band appeared to dominate, its formation was much more gradual than in biaxial tests, and relatively diffuse shear persisted in the conjugate direction well after peak stress.

It appears that shear banding naturally tends to initiate along conjugate planes. The differences in patterns of shear band formation between biaxial and triaxial tests arise at least partially from the differences in boundary conditions. When boundary conditions do not impose constraints on specimen behavior, as in the biaxial apparatus, an evolution to one dominant, persistent, nearly linear shear band is favored. That the shear band in the triaxial test had not developed as abruptly as in the biaxial specimens is likely a consequence of the deformational constraints induced by the laterally fixed, unlubricated top and bottom soil-platen boundaries.

DIC analyses performed over closely spaced image increments help clarify how a persistent shear band forms. Figure 3 shows displacements determined during a biaxial compression test on dense Delaware beach sand. Axes indicate distances along the specimen analysis area in image

coordinate space (origin at upper left of image). In the first image increment, which immediately preceded peak stress (4.75% axial strain), localized shear appears to be initiating in two places: at image coordinates y = -80 mm and y = -110 mm. The next increment encompassed peak stress (4.75% axial strain), and only one persistent shear band, partially formed, is seen. Within the final increment, between 0.09 and 0.25% axial strain following peak stress, the shear band has entirely formed (analyses in subsequent increments indicated complete formation).

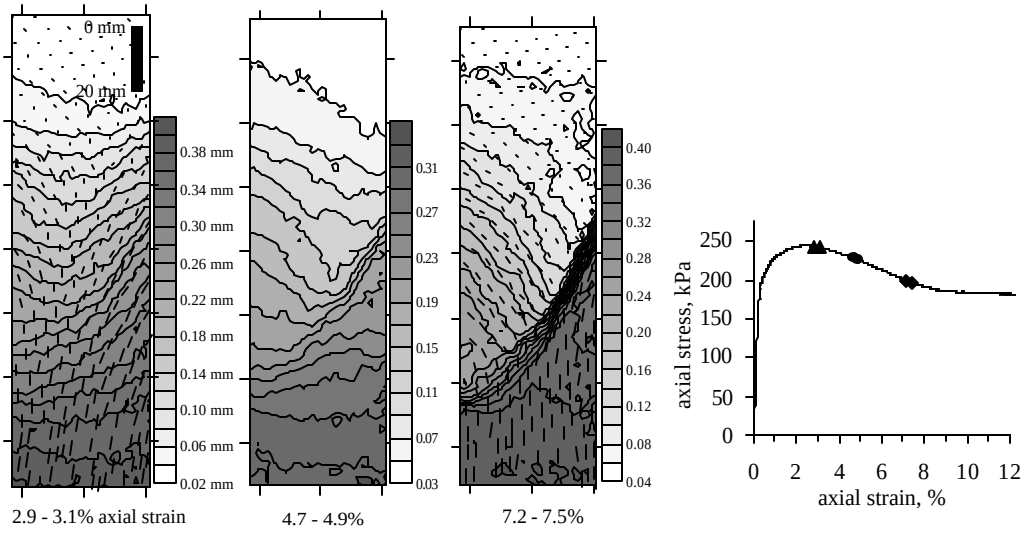

Figure 2. Local Displacements and Global Behavior During Triaxial Test on Levering Sand.

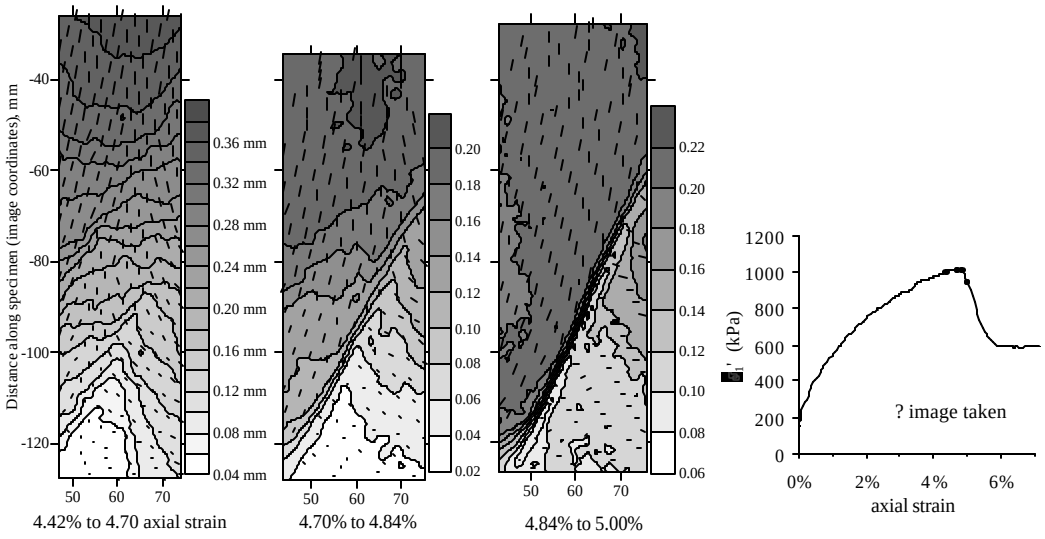

Figure 3. Local Displacements During Biaxial Compression Test on Delaware Beach Sand.

Shear bands thus seem to initiate from the sides of the specimen, where the least deformational constraint exists. In a uniform sand, shear band formation was quite abrupt. The shear band formed between 0.1 and 0.25% axial strain after peak stress was achieved, during which time about 0.25 mm of differential movement occurred across the shear band. More than one conjugate pair of shear bands appeared to be forming initially, but due to the nature of the boundary conditions, formation of only one persistent shear band was favored.

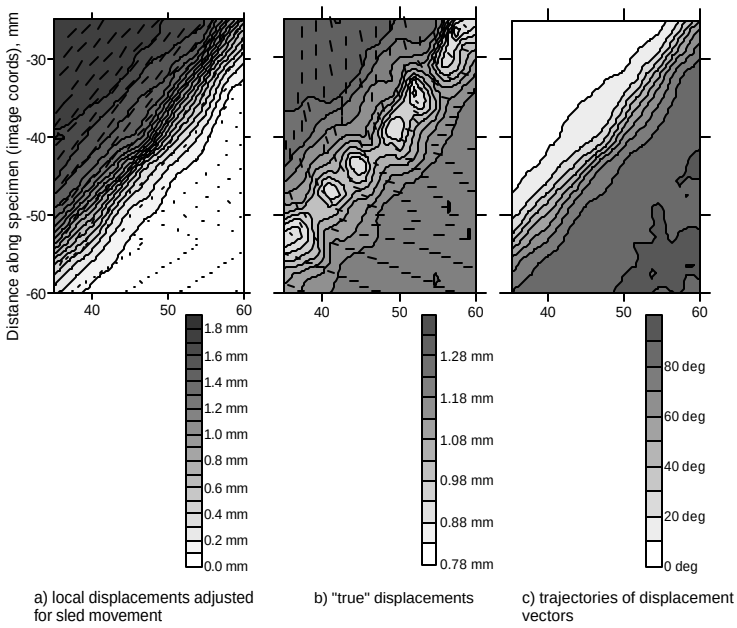

Figure 4. Displacements in a Fully Formed Shear Band during Biaxial Testing of Concrete Sand.

3.2 Displacement Patterns Within Persistent Shear Bands

Figure 4 shows displacements within a persistent shear band during biaxial compression of a medium dense concrete sand. Figure 4a shows the "adjusted" specimen displacements, obtained by subtracting out the sled movements measured during the image increment. Due to the more well-graded nature of this sand, the shear band was wider and wavier than in more uniform sands (see Figures 1 and 3). Displacement gradients, while evidently parabolic across the width of the shear band, appear to be constant along the length of a shear band, with minor fluctuations only.

However, when the "true" displacements, those unadjusted for sled movement, are viewed (Figure 4b), the data reveal coherent "cells" of lower displacement magnitude periodically located along the length of the shear band. These same "structures" were seen in more uniform sands as well (Figure 1). The trajectory of the displacement vectors is shown in Figure 4c (zero degrees indicates displacement oriented vertically downward). It appears that the sand at a given position across the width of a shear band is moving in the same direction, just some of it is moving faster. Such periodicity in displacement field has been suggested to occur for sands (Oda and Kazama [13]), and was attributed to build-up and collapse of grain "columns" along the shear band. Periodicity also has been observed in DEM-based granular material simulations (e.g. Williams and Rege [14]), and has been attributed to stiffness fluctuations due to material heterogeneity (Gaspar and Koenders [15]).

4 CONCLUSIONS

Displacements have been measured locally, to a high degree of accuracy, within dilative sand specimens throughout biaxial and triaxial compression using the technique of Digital Image Correlation (DIC). Analyses of local displacement data revealed the following:

1. Shear bands naturally tend to initiate along conjugate planes. Test boundary conditions dictate whether single or multiple shear bands will evolve.
2. Strain localization initiates near the unconstrained edges of a specimen.
3. Shear bands form somewhat abruptly, but not instantaneously. For the case of a uniform sand, around 0.25 mm of shear displacement occurred before the band was entirely formed.
4. Displacement gradients across a shear band are nonlinear. Displacement fields along the length of a shear band exhibit notable periodicity, possibly associated with build-up and collapse of "force chains".

5 REFERENCES

[1] Harris, W.W., G. Viggiani, M.A. Mooney, and R.J. Finno, "Use of Stereophotogrammetry to Analyze the Development of Shear Bands in Sand", *Geotechnical Testing J*, 18 (4), 405-420, 1995.

[2] Finno, R.J., W.W. Harris, M.A. Mooney and G. Viggiani, "Shear Bands in Plane Strain Compression of Loose Sand", *Geotechnique*, 47 (1), 149-165, 1997.

[3] Desrues, J., R. Chambon, M. Mokni and F. Mazerolle, "Void Ratio Evolution Inside Shear Bands in Triaxial Sand Specimens Studied by Computed Tomography", *Geotechnique*, 46 (3), 529-546, 1996.

[4] Liang, L., A. Saada, J.L. Figueroa, and C.T. Cope, "The Use of Digital Image Processing in Monitoring Shear Band Development", *Geotechnical Testing J*., 20 (3), 324-339, 1997.

[5] Mooney, M.A., G. Viggiani, and R. J. Finno, "Undrained Shear Band Deformation in Granular Media," *J. of Engineering Mechanics*, 123 (6), 577-585, 1997.

[6] Finno, R.J. and A.L. Rechenmacher, "Effects of consolidation History on Critical State of Sand, *J. of Geotechnical and Geoenvironmental Engineering*, 129 (4), 350-360, 2003.

[7] Han, C. and A. Drescher, "Shear Bands in Biaxial Tests on Dry Coarse Sand", *Soils and Foundations*, 33 (1), 118-132, 1993.

[8] Alshibli, K.A., S. N. Batiste, and S. Sture, "Strain Localization in Sand: Plane strain versus Triaxial Compression," *J. of Geotechnical and Geoenvironmental Engineering*, 129 (6), 483-494, 2003.

[9] Rechenmacher, A.L. and R.J. Finno, "Digital image Correlation to Evaluate Shear Banding in Dilative sands," *Geotechnical Testing J*., 27 (1), 13-22, 2004.

[10]Drescher, A., I. Vardoulakis, and C. Han, "A Biaxial Apparatus for Testing Soils," *Geotechnical Testing J*., 13 (30, 226-234, 1990.

[11] Sutton, M.A., S.R. McNeill, J.D. Helm, and Y.J. Chao, "Advances in Two-Dimensional and Three-Dimensional Computer Vision," Photomechanics, Topics in Applied Physics, Vol 77, 323-372, 2000..

[12] Helm, J.D., McNeill, S.R. and Sutton, M.A., "Improved 3-D image correlation for surface displacement measurement, *Optical Engineering*, 35 (7), 1911-1920, 1996.

[13] Oda, M. and H. Kazama, "Microstructure of Shear Bands and its Relation to the Mechanisms of Dilatancy and Failure of Dense Granular Soils", *Geotechnique*, 48 (4), 465-481, 1998.

[14] Williams, J.R. and N. Rege, "Coherent vortex structures in deforming granular materials," *Mechanics of Cohesive-Frictional Materials*, Vol. 2, 1997

[15] Gaspar, N. and M.A. Koenders, "Micromechanic Formulation of Macroscopic Structures in a Granular Medium," *J. of Engineering Mechanics*, 127 (10), 987-993, 2001.